Phytochemistry 220 (2024) 114020

Contents lists available at ScienceDirect

Phytochemistry

journal homepage: www.elsevier.com/locate/phytochem

Aporphine alkaloids and a naphthoquinone derivative from the leaves of *Phaeanthus lucidus* Oliv. and their α-glucosidase inhibitory activity

Passakorn Teerapongpisan [a], Virayu Suthiphasilp [b], Pakit Kumboonma [c], Tharakorn Maneerat [a,d], Thidarat Duangyod [d,e], Rawiwan Charoensup [d,e], Phunrawie Promnart [f], Surat Laphookhieo [a,d,*]

[a] Center of Chemical Innovation for Sustainability (CIS) and School of Science, Mae Fah Luang University, Chiang Rai, 57100, Thailand
[b] Department of Industrial Technology and Innovation Management, Faculty of Science and Technology, Pathumwan Institute of Technology, Bangkok, 10330, Thailand
[c] Department of Applied Chemistry, Faculty of Science and Liberal Arts, Rajamangala University of Technology Isan, Nakhon Ratchasima, 30000, Thailand
[d] Medicinal Plant Innovation Center of Mae Fah Luang University, Chiang Rai, 57100, Thailand
[e] School of Integrative Medicine, Mae Fah Luang University, Chiang Rai, 57100, Thailand
[f] School of Science, Mae Fah Luang University, Chiang Rai, 57100, Thailand

ARTICLE INFO

Keywords:
Phaeanthus lucidus
Annonaceae
Aporphine alkaloids
Naphthoquinone
α-Glucosidase inhibitory activity

ABSTRACT

Three previously undescribed aporphine alkaloids, phaeanthuslucidines E–G, one previously undescribed naphthoquinone derivative, phaeanthusnaphthoquinone, and three known compounds were isolated from an EtOAc extract of the leaves of *Phaeanthus lucidus* Oliv. The structures of all previously undescribed compounds were established through extensive spectroscopic investigations and high-resolution mass spectroscopy. The 6a*R* configuration of phaeanthuslucidines E–G was assigned by comparing their ECD spectra and specific rotation values with the reported known compounds. Some isolated compounds were evaluated for their α-glucosidase inhibitory activity. Among these compounds, phaeanthuslucidine E showed the highest α-glucosidase inhibitory activity with an IC_{50} value of 17.9 ± 0.4 μM. The molecular docking of phaeanthuslucidine E was further studied.

1. Introduction

The *Phaeanthus* genus, a member of the Annonaceae family, encompasses a plethora of over 20 distinct species, predominantly distributed across the continents of Asia (Nhiem et al., 2017). Many species in the genus *Phaeanthus* have been used to treat infectious, gastrointestinal, inflammatory, and dermatitis diseases (Magpantay et al., 2021; Tu et al., 2022). *Phaeanthus* species produced alkaloids as major compounds (Johns et al., 1968; Sedmera et al., 1990; Atan et al., 2011; Zaima et al., 2012; Nhiem et al., 2017; Magpantay et al., 2021; Malaluan et al., 2022; Tu et al., 2022); lignans and terpenoids were observed as minor compounds (Nhiem et al., 2017). Many compounds found in *Phaeanthus* species exhibited diverse biological activities, including anti-inflammatory (Nhiem et al., 2017; Magpantay et al., 2021; Tu et al., 2022), anti-microbial (Sedmera et al., 1990; Magpantay et al., 2021; Malaluan et al., 2022), and anti-cancer (Malaluan et al., 2022). *Phaeanthus lucidus* Oliv. (Synonym name *P. splendens*) is an evergreen shrub that is distributed throughout the evergreen forests of Thailand (Wiya et al., 2021). In previous reported phytochemical investigations (Teerapongpisan et al., 2023), five dimeric aporphine alkaloids were found from the twig extract of this plant, and four of these compounds were scalemic mixtures, which were successfully resolved by chiral HPLC. Some aporphine alkaloids isolated from *P. lucidus* displayed α-glucosidase inhibitory activity with IC_{50} values in the range of 6.7–29.2 μM (Teerapongpisan et al., 2023). To complete the phytochemical investigation of this plant as well as continue the investigation of the α-glucosidase inhibitory activity of the natural products obtained, three previously undescribed aporphine alkaloids (**1**–**3**), one previously undescribed naphthoquinone derivative (**7**), and three known compounds (**4**–**6**) were isolated from the leaf extract of this plant (see Fig. 1). The anti-diabetic property of some isolated compounds was evaluated by their inhibition of yeast α-glucosidase. The molecular docking simulation of the active compound was also studied.

2. Results and discussion

The EtOAc extract of *P. lucidus* leaves was separated using various chromatographic methods, yielding three previously undescribed aporphine alkaloids (**1**–**3**) and one previously undescribed naphthoquinone derivative (**7**), together with three previously reported ones

* Corresponding author. Center of Chemical Innovation for Sustainability (CIS) and School of Science, Mae Fah Luang University, Chiang Rai, 57100, Thailand.
E-mail address: surat.lap@mfu.ac.th (S. Laphookhieo).

https://doi.org/10.1016/j.phytochem.2024.114020
Received 19 November 2023; Received in revised form 11 February 2024; Accepted 12 February 2024
Available online 15 February 2024

(**4**–**6**). These previously reported compounds were identified as *N*-acetylxylopine (**4**) (Nonato et al., 1990), *N*-acetylanonaine (**5**) (Nonato et al., 1990), and corydaldine (**6**) (Atan et al., 2011) by comparison of their NMR spectroscopic data with reported in the literature.

2.1. Structural elucidation

Compounds **1**–**3** were aporphine alkaloids, which showed the common IR spectra for hydroxy and amide carbonyl functionalities at ca. 3413 and 1677 cm^{-1}, respectively. The UV–vis spectra of these compounds showed the maxima absorption bands at 206, 241, 285, and 324 nm. The structures of compounds 1–3 shared the same core structure as compounds **4** and **5**. However, the key difference was that the structures of compounds **4** and **5** displayed the *N*-acetyl group, but the structures of compounds **1**–**3** were *N*-benzoyl derivatives.

Compound **1**, phaeanthuslucidine E, was isolated as a yellow amorphous powder. Its molecular formula was determined to be $C_{26}H_{23}NO_6$ by HRESIMS (*m/z* 446.1583; $[M + H]^+$, calcd for 446.1598). The ^1H and ^{13}C NMR (Table 1) of compound 1 displayed the resonances for aporphine unit similar to those of *N*-acetylxylopine (4) (Nonato et al., 1990; Lo et al., 2000), including an ABX spin system [δ_H 8.05 (1H, d, J = 9.1 Hz)/δ_C 128.5, C-11, δ_H 6.90 (1H, dd, J = 9.1, 2.4 Hz)/δ_C 112.5, C-10, and δ_H 6.91 (1H, d, J = 2.4 Hz)/δ_C 113.8, C-8], a singlet aromatic proton [δ_H 6.64 (1H, s)/δ_C 106.6, C-3], one methine proton [δ_H 5.15 (1H, dd, J = 14.1, 4.2 Hz)/δ_C 51.0, C-6a], three methylene protons [δ_H 2.84 (1H, overlap), H-4β and δ_H 2.67 (1H, dd, J = 15.7, 2.4 Hz), H-4α/δ_C 30.4, C-4, δ_H 4.17 (1H, dd, J = 12.2, 3.4 Hz), H-5β and δ_H 3.29 (1H, td, J = 12.2, 2.4 Hz), H-5α/δ_C 42.6, C-5, and δ_H 3.19 (1H, dd, J = 14.1, 4.2 Hz), H-7β and δ_H 2.95 (1H, overlap), H-7α/δ_C 34.2, C-7], one methylenedioxy group [δ_H 6.13 (1H, d, J = 1.0 Hz) and δ_H 6.03 (1H, d, J = 1.0 Hz)/δ_C 100.9, 1-OCH_2O-2], and one methoxy group [δ_H 3.85 (3H, s)/δ_C 54.7, 9-OMe]. At the *N*-substituent unit, compound 1 displayed a set of 4-hydroxy-3-methoxy benzoyl unit ([δ_H 7.09 (1H, d, J = 1.8 Hz)/δ_C 110.9, C-3′, δ_H 6.98 (1H, dd, J = 8.0, 1.8 Hz)/δ_C 120.1, C-7′, and δ_H 6.89 (1H, d, J = 8.0 Hz)/δ_C 114.6, C-6′] and one methoxy group [δ_H 3.90 (3H, s)/δ_C 55.5, 4′-OMe]) instead of the acetyl group as appeared in compound 4. The ^1H NMR resonances of H-6a and H-5β were shifted downfield due to the anisotropic effect of the adjacent carbonyl group of the benzoyl derivative compared to the *N*H (δ_H 3.71 to 4.32 for H-6a and δ_H 2.87 to 3.73 for H-5) (Nguyen et al., 2008; Tsai et al., 2008; Guo et al., 2011; Yu et al., 2019; Chaichompoo et al., 2021)) or *N*R (δ_H 4.46 to 5.45 for H-6a and δ_H 2.70 to 4.98 for H-5) (Yu et al., 1998; Chang et al., 2000; Pabon et al., 2010; Chen et al., 2011; Zheng et al., 2021; Liu et al., 2023)) substitutions. This information suggested that the 4-hydroxy-3--methoxy benzoyl unit is linked to the *N* atom. The significant NOESY cross-peaks between H-5β with H-3′ confirmed this assignment. The full assignments of ^1H and ^{13}C resonances were confirmed by ^1H–^1H COSY (Fig. 2), HSQC, HMBC (Fig. 2), and NOESY (Fig. 3).

The relative configuration of C-6a was determined by NOESY experiments. Key NOESY cross-peaks (Fig. 3) between H-4β/H-6a and H-6a/H-7β indicated H-4β, H-6a, and H-7β located at the same side and assigned as the β-orientation. The absolute configuration of C-6a of compound **1** was assessed by comparing the ECD data and specific rotation with the reported known compounds in the literature. The 6a*R* and 6a*S* configurations have been found in nature which displayed the ECD spectra with the positive Cotton effect at ca. 273 nm and a negative Cotton effect at ca. 237 nm for the 6a*R* configuration displayed (Ringdahl et al., 1981; Guo et al., 2011; Chaichompoo et al., 2021), whereas the 6a*S* configuration showed the opposite ECD spectra at the same range (Ringdahl et al., 1981; Chen et al., 2011; Matsushige et al., 2012; Chaichompoo et al., 2021). In addition, the specific rotation of the 6a*R* configuration was levorotatory, and the 6a*S* configuration was dextrorotatory. Compound **1** gave a positive Cotton effect at 273 nm and a negative Cotton effect at 237 nm (Fig. 4), and its specific rotation was levorotatory ($[\alpha]_D^{25}$ −87), which was well matched with the 6a*R* configuration. Compound 1 was, therefore, identified as having the *R* configuration and was named (−)-(6a*R*)-phaeanthuslucidine E.

Compound **2** was obtained as a brown amorphous powder. The HRESITOFMS data (*m/z* 476.1705 $[M + H]^+$) corresponded to the molecular formula $C_{27}H_{25}NO_7$. The spectroscopic data of compound **2**, including UV, IR, ^1H, and ^{13}C NMR data (Table 1), were closely related to those of compound **1**. Compound **2** showed resonances for a tetra-substituted benzene ring [δ_H 6.79 (2H, s, H-3′ and H-7′)/δ_C 104.6] and two methoxy groups [δ_H 3.88 (6H, s, 4′-OMe and 6′-OMe)/δ_C 55.9] instead of the ABX aromatic protons coupling pattern for H-3′, H-6′, and H-7′ of benzoyl unit found in compound **1**. The correlations of H-3′ and H-7′ with C-4′ and C-6′ (δ_C 147.6) in the HMBC spectrum of compound **2**, together with the NOESY correlations between H-3′/4′-OMe and H-7′/6′-OMe, supported the position of methoxy groups at C-4′ and C-6′. The specific rotation and ECD spectra (Fig. 4) of compound **2** were similar to those of compound **1**. Thus, the absolute configuration of compound **2** was assigned as 6a*R* and was named as (−)-(6a*R*)-phaeanthuslucidine F.

Compound **3**, HRESITOFMS *m/z* 416.1494 $[M + H]^+$ ($C_{25}H_{21}NO_5$), was isolated as a yellow amorphous powder. The ^1H and ^{13}C NMR data (Table 1) obtained for compound **3** were similar to those of compound **1**. The main difference was the aromatic proton spin system on the

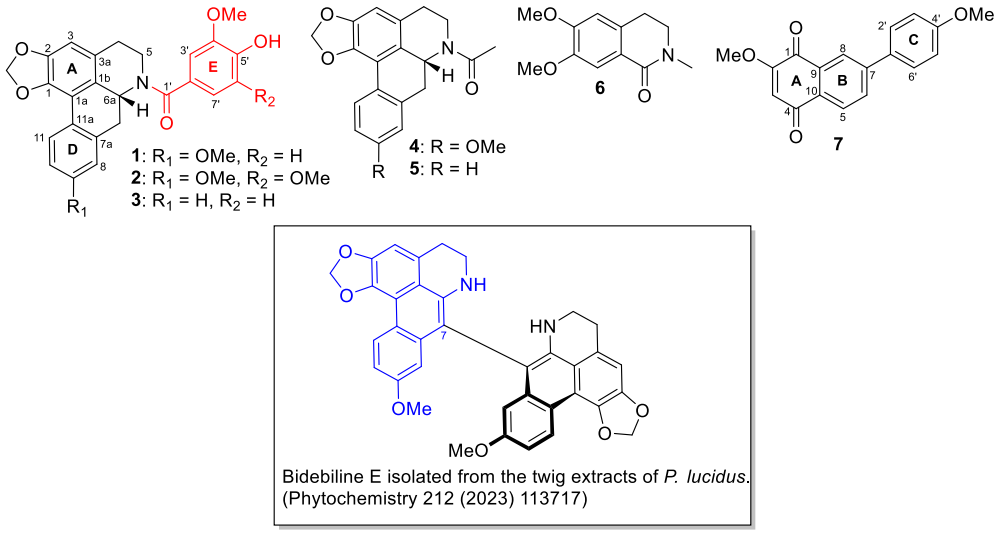

Fig. 1. Isolated compounds from the leaves of *P. lucidus*.

Table 1
^{1}H and ^{13}C NMR Spectroscopic Data of compounds **1**–**3** in acetone-d_6.

Position	**1**[a]	δ_H, mult (*J* in Hz)	**2**[b]	δ_H, mult (*J* in Hz)	**3**[b]	δ_H, mult (*J* in Hz)
	δ_C		δ_C		δ_C	
1	142.4	–	142.3	–	143.1[c]	–
1a	117.1	–	117.1	–	117.0	–
1 b	125.1	–	125.1[c]	–	125.8[c]	–
2	146.9	–	146.9	–	147.1[c]	
3	106.6	6.64 s	106.6	6.64 s	107.5	6.71 s
3a	127.9	–	127.9[c]	–	127.9[c]	–
4	30.4	2.84 overlap; 2.67 dt (15.7, 2.4)	30.3[c]	2.87 overlap; 2.68 dt (15.6, 2.4)	30.4[c]	2.84 overlap; 2.69 dt (15.5, 2.2)
5	42.6	4.17 dd (12.2, 3.4); 3.29 td (12.2, 2.4)	42.3[c]	4.19 dd (11.7, 2.7); 3.30 m	41.3[c]	4.19 dd (13.4, 3.1); 3.31 td (13.4, 2.2)
6a	51.0	5.15 dd (14.1, 4.2)	51.1[c]	5.15 dd (14.0, 4.4)	51.1[c]	5.17 dd (14.0, 4.3)
7	34.2	3.19 dd (14.1, 4.2); 2.95 overlap	34.2[c]	3.21 dd (14.0, 4.4); 2.94 overlap	33.8[c]	3.23 dd (14.0, 4.3); 2.94 overlap
7a	138.0	–	138.0	–	136.1	–
8	113.8	6.91 d (2.4)	113.8	6.92 d (2.6)	128.6	7.33 m
9	159.4	–	159.4[c]	–	127.8	7.28 m
10	112.5	6.90 dd (9.1, 2.4)	112.4	6.91 dd (9.4, 2.6)	126.9	7.33 m
11	128.5	8.05 d (9.1)	128.6	8.05 d (9.4)	127.1	8.13 d (9.1)
11a	123.3	–	123.3[c]	–	127.9[c]	–
1-OCH_2O-2	100.9	6.13 d (1.0); 6.03 d (1.0)	100.9	6.13 d (1.1); 6.03 d (1.1)	101.1	6.17 d (1.0); 6.05 d (1.0)
9-OMe	54.7	3.85 s	54.7	3.85 s	–	–
1′	169.9	–	169.9[c]	–	169.9[c]	–
2′	128.5	–	127.4[c]	–	128.6[c]	–
3′	110.9	7.09 d (1.8)	104.6	6.79 s	110.9	7.10 d (1.8)
4′	147.4	–	147.6	–	147.3[c]	–
5′	147.9	–	137.2[c]	–	147.7[c]	–
6′	114.6	6.89 d (8.0)	147.6	–	114.6[c]	6.89 d (8.0)
7′	120.1	6.98 dd (8.0, 1.8)	104.6	6.79 s	120.2	6.99 dd (8.0, 1.8)
4′-OMe	55.5	3.90 s	55.9	3.88 s	55.5	3.90 s
6′-OMe	–	–	55.9	3.88 s	–	–

[a] ^{1}H NMR at 125 MHz and ^{13}C NMR at 500 MHz.
[b] ^{1}H NMR at 150 MHz and ^{13}C NMR at 600 MHz.
[c] Assignments from HSQC and HMBC data.

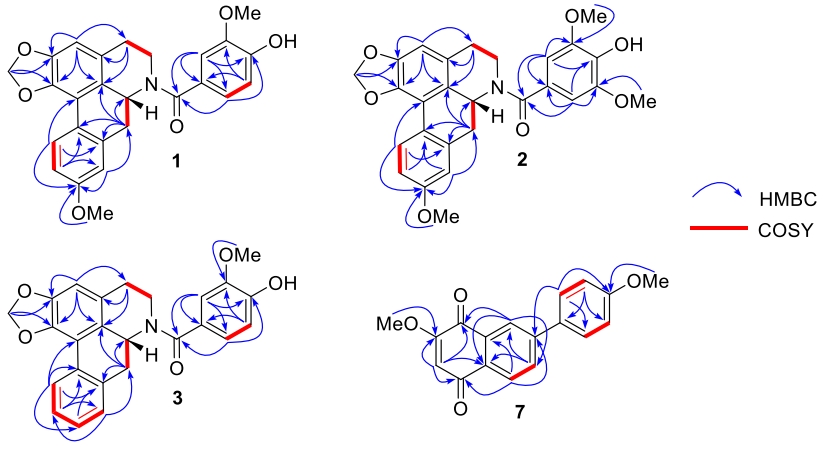

Fig. 2. ^{1}H–^{1}H COSY (red, bold) and selected HMBC (blue single arrows) correlations of compounds **1**–**3** and **7**. (For interpretation of the references to color in this figure legend, the reader is referred to the Web version of this article.)

aporphine alkaloid unit. Compound 3 displayed resonances for a 1,2-disubstituted benzene ring [δ_H 8.13 (1H, d, J = 9.1 Hz)/δ_C 127.1, C-11, δ_H 7.33 (1H, m)/δ_C 128.6, C-8, δ_H 7.33 (1H, m)/δ_C 126.9, C-10, and δ_H 7.28 (1H, m)/δ_C 127.8, C-9], whereas compound 1 showed an ABX aromatic proton coupling pattern for H-8, H-10, and H-11 and a methoxy signal. The structure of compound 3 was confirmed by HMBC data as shown in Fig. 2. The ECD spectrum of compound **3** (Fig. 4) and its specific rotation ($[\alpha]_D^{25}$ −56) were similar to those of compounds **1** and **2**, suggesting the absolute configuration was 6a*R* configuration. Thus, the structure of compound **3**, (−)-(6a*R*)-phaeanthuslucidine G, was assigned.

Compound **7** was isolated as a yellow amorphous powder. Its molecular formula, $C_{18}H_{14}O_4$, was deduced from HRESIMS. The UV spectrum showed absorption bands at λ_{max} 234, 276, and 312 nm, and the IR spectrum indicated two carbonyl (1724 and 1647 cm^{-1}) and aromatic (1519 and 1454 cm^{-1}) functionalities, indicative of a naphthalene skeleton (Wu et al., 2011; Auranwiwat et al., 2017; Salae et al., 2017). The ^{13}C NMR data of compound **7** displayed 18 resonances assigned to eight aromatic methine carbons, two methoxy carbons, two carbonyl carbons, and six non-protonated aromatic carbons. The ^{1}H and ^{13}C NMR data (Table 2) demonstrated resonances of the phenyl naphthoquinone skeleton as follows: a set of ABX pattern [δ_H 8.25 (1H, d, J = 1.4 Hz)/δ_C 123.4, C-8, δ_H 8.10 (1H, dd, J = 8.1, 1.4 Hz)/δ_C 131.5, C-6, and δ_H 8.07 (1H, d, J = 8.1 Hz)/δ_C 126.5, C-5], four aromatic protons of a *para*-disubstitued benzene ring [δ_H 7.77 (2H, d, J = 8.8 Hz)/δ_C 128.4, C-2′/C-6′ and δ_H 7.11 (2H, d, J = 8.8 Hz)/δ_C 114.6, C-3′/C-5′], one singlet aromatic proton [δ_H 6.28 (1H, s)/δ_C 109.8, C-3], and two methoxy

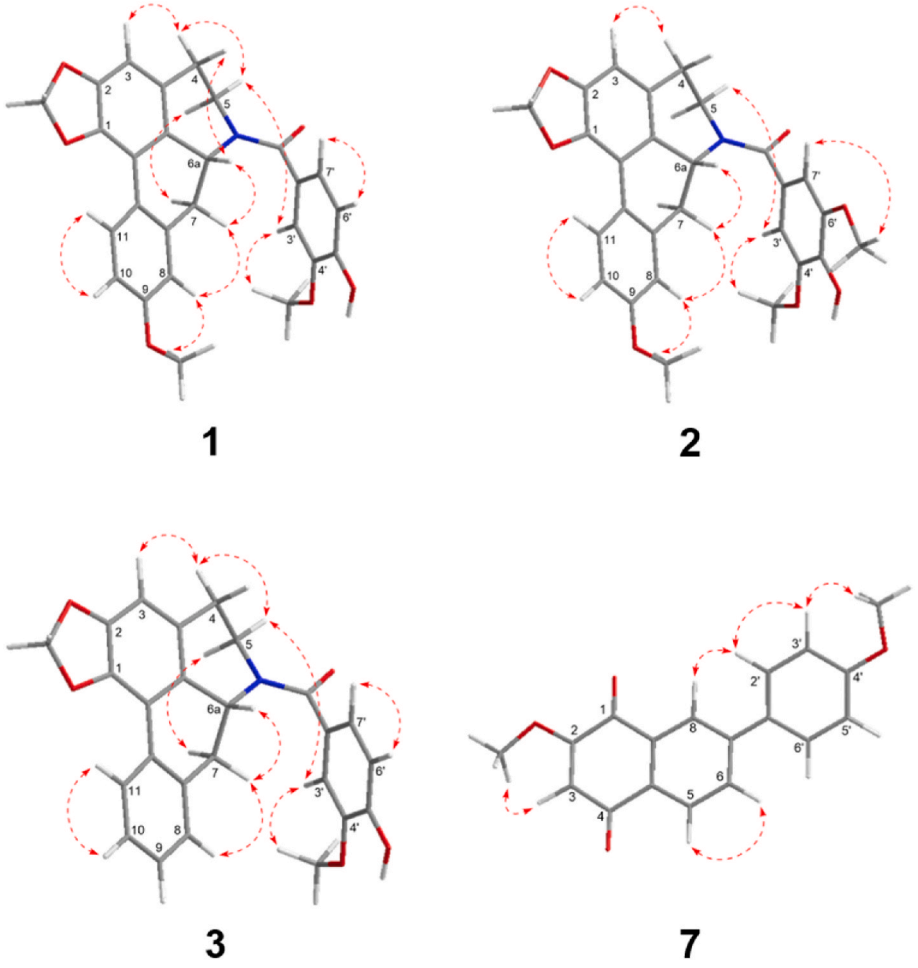

Fig. 3. Key NOESY (red dashed arrows) correlations of compounds 1−3 and 7. (For interpretation of the references to color in this figure legend, the reader is referred to the Web version of this article.)

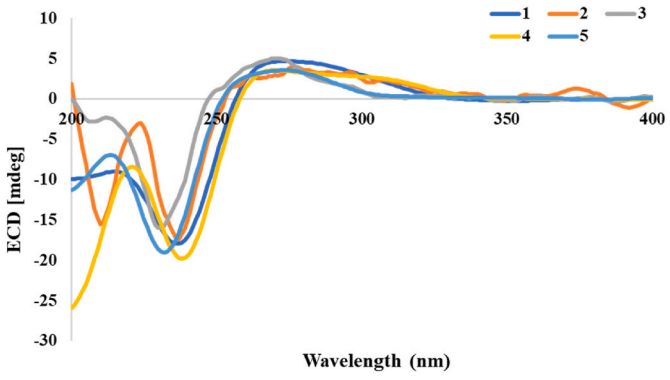

Fig. 4. Experimental ECD spectra (MeOH) of compounds (−)-(**1**), (−)-(**2**), (−)-(**3**), (−)-(**4**), and (−)-(**5**).

groups [δ_H 3.95 (3H, s)/δ_C 56.0, 2-OMe and δ_H 3.88 (3H, s)/δ_C 54.9, 4′-OMe]. The typical carbonyl groups were confirmed by HMBC correlations (Fig. 2) between H-8 and C-1 (δ_C 179.6) and H-5 and C-4 (δ_C 184.0), demonstrating that the other two carbonyl groups located at C-1 and C-4, respectively. The *para*-disubstituted aromatic ring was located at C-7 (δ_C 145.4) of the naphthalene-1,4-dione unit (ring B) according to the HMBC correlations of the aromatic protons H-2′ and H-6′ with C-7. The two methoxy groups were placed at C-2 and C-4′, which supported the assignments by the HMBC correlations as follows: H-3 and 2-OMe with C-2 (δ_C 160.8) and H-2′, H-6′, and 4′-OMe with C-4′ (δ_C 160.6).

Table 2
^{1}H (500 MHz) and^{13}C (150 MHz) NMR Spectroscopic Data of compound **7** in acetone-d_6.

Position	**7**	
	δ_C	δ_H, mult (*J* in Hz)
1	179.6	–
2	160.8	–
3	109.8	6.28 s
4	184.0	–
5	126.5	8.07 d (8.1)
6	131.5	8.10 dd (8.1, 1.4)
7	145.4	–
8	123.4	8.25 d (1.4)
9	131.8	–
10	130.2	–
1′	131.0	–
2′/6′	128.4	7.77 d (8.8)
3′/5′	114.6	7.11 d (8.8)
4′	160.6	–
2-OMe	56.0	3.95 s
4′- OMe	54.9	3.88 s

The observation of NOESY cross-peaks (Fig. 3) between H-3 and 2-OMe and between H-3′, H-5′, and 4′-OMe also confirmed these assignments. Compound **7**, therefore, was named as phaeanthusnaphthoquinone (2-methoxy-7-(4-methoxyphenyl)naphthalene-1,4-dione).

2.2. α-Glucosidase inhibitory activities and in silico molecular docking

Only compounds with sufficient quantity (**1** and **4**–**7**) were evaluated for their α-glucosidase inhibitory activities by the colorimetric assay. Of these, compound **1** displayed good α-glucosidase inhibitory activity with an IC_{50} value of 17.9 ± 0.4 μM, which was better than that of acarbose, a positive control (IC_{50} value of 184.9 ± 0.9 μM); however, all remaining were found to be inactive. It should be noted that the structures of **1**, **4**, and **5** were mainly different at the *N*-substitution. Compound **1** contained the *N*-benzoyl unit, which seems to play an important role in α-glucosidase inhibitory activity compared to the *N*-acyl group in structures **4** and **5**. To confirm this assumption, compounds **1**, **4**, and **5** were further studied on the *in silico* molecular docking (Table 3), which was performed to examine the potential interactions of these compounds with the α-glucosidase (PDB ID: 2QMJ). It was found that compound **1** had the lowest free binding energy (−8.89 kcal/mol). In the case of hydrophilic interactions, the hydrogen atom of the phenolic group of compound **1** showed hydrophilic interactions with the carbonyl oxygen of Arg202 (2.10 Å) in the active site residue (Fig. 5A). Furthermore, four π-π aromatic ring interactions and five van der Waals force effects were observed in compound 1. These interactions included aromatic rings with Tyr299 (5.11 Å), Phe575 (5.15 Å, 5.43 Å), Trp406 (5.27 Å) and hydrogen atoms of the methoxy group with Gln603 (2.34 Å, 2.86 Å), Ser448 (2.40 Å) and hydrogen atoms of methylene groups with Asp203 (2.40 Å) and Tyr299 (2.75 Å). Undoubtedly, the docking score (−6.98 kcal/mol for **4** and (−7.38 kcal/mol for **5**) (Table 3) and the lack of significant interaction between the 4-hydroxy on benzoyl unit and ligand afford the weak binding (Fig. 5B and C). The results showed that the hydroxy group of the benzoyl unit could be introduced into the active site of the α-glucosidase and block the catalytic reaction by interacting with the entrance of α-glucosidase. This information could explain why compounds 4 and 5 had less α-glucosidase inhibitory activity than compound 1.

It is interesting to note that in a previous study, bidebiline E, an aporphine alkaloid isolated from the same plant (Teerapongpisan et al., 2023), displayed remarkably high α-glucosidase inhibitory activity (IC_{50} = 6.8 ± 0.3 μM) comparing to that of compound **1** (IC_{50} = 17.9 ± 0.4 μM). This suggests that the different structures of bidebiline E and compound **1** could play an important role in α-glucosidase inhibitory activity. The structure of compound **1** was a monomeric $\Delta^{6a(7)}$ dihydroaporphine alkaloid and the *N*-substitution group was a benzoyl derivative. In contrast, bidebiline E was a dimeric $\Delta^{6a(7)}/\Delta^{6'a(7')}$ dehydroaporphine alkaloid with free *NH/NH'* groups that are essential to increase the α-glucosidase inhibitory activity.

3. Conclusions

In conclusion, four previously undescribed compounds, including three aporphine alkaloids (**1**–**3**) and one naphthoquinone derivative (**7**), together with three known compounds (**4**–**6**), were obtained from the leaf extract of *P. lucidus*. Their structures were deduced by spectroscopic method and ECD data. Some isolated compounds were evaluated to derive their inhibitory effects on the α-glucosidase. Interestingly, compound 1, having a trisubstituted benzoyl unit, exhibited a significant inhibitory effect. A molecular docking simulation was employed to disclose possible interaction mechanisms of compound **1** with α-glucosidase. Our findings provided insights into the hypoglycemic activity of this plant.

Table 3
In silico α-Glucosidase Inhibitory Activities of compounds **1**, **4**, and **5**.

Compounds	Binding affinity		Hydrophilic interactions (Hydrogen bonding)	Hydrophobic interactions
	ΔG (kcal/mol)	K_i (*μ*M)		
1	−8.89	0.3	Arg202	Gln603, Asp 327, Ser448, Asp203, Tyr299, Trp406, Phe575, Asp 542
4	−6.98	7.66	–	Asp443, Met444, Tyr605, Trp406, Phe450, Gln603. Tyr299, Phe575
5	−7.38	3.93	–	Asp443, Met444, Trp406, Phe450, Tyr299, Phe575

4. Experimental

4.1. General experimental procedures

Optical rotations were measured on a JASCO P-2000 polarimeter. UV Spectra were recorded on a VARIAN cary 5000 spectrophotometer, and CD spectra were obtained using a JASCO J-1500 spectrometer. IR Spectra were obtained using a PerkinElmer FTS FT-IR spectrometer. HRESIMS and HRESITOFMS data were measured on an Agilent 1290 infinity II/G6545B QTOF mass spectrometer and a Kratos MS-50 mass spectrometer, respectively. HPLC was performed using an Agilent Technology HPLC 1260 Infinity II system, coupled to a 1260 Infinity II Diode Array Detector HS and equipped with a C-18 column. NMR spectra were run on 500 MHz Bruker AV-500 and 600 MHz Bruker AV-600 spectrometers. Column chromatography (CC) was performed on Silica gel C60 (0–20 μm, SiliCycle® Inc.), Sephadex LH-20. Fractions and isolated compounds were monitored by thin-layer chromatography (TLC), and spots were observed by ultraviolet (UV) light (254 and 310 nm).

4.2. Plant material

The leaves of *P. lucidus* were collected in April 2021 from Narathiwat Province (N: 6.156754°, E: 101.664661°), Thailand. The plant was identified by Mr. Abdulromae Baka (Independent Research Group on Plant Diversity in Thailand, Sichon, Nakhon Si Thammarat, 80120, Thailand), and a voucher specimen (MFUNPR0210) was deposited at the Natural Products Research Laboratory, School of Science, Mae Fah Luang University.

4.3. Extraction and isolation

The chopped and air-dried leaves of *P. lucidus* (3.8 kg) were extracted with EtOAc (3 × 20 L) at room temperature and concentrated under reduced pressure to provide an EtOAc extract (60.2 g). This crude extract was subjected to a C_{18} reverse-phase silica gel CC eluted with MeOH–H_2O (1:4 v/v) to afford three fractions (Fr. PLL1–PLL3). Separation of fraction PLL1 (175.7 mg) using CC over silica gel (2:3 v/v, EtOAc−hexanes) yielded compound **6** (2.7 mg). Fraction PLL3 (281.3 mg) was fractionated over a Sephadex-LH20 eluted with MeOH (100% v/v) to provide seven subfractions (Fr. PLL3A–PLL3G). Compounds **3** (0.7 mg, t_R 46.4 min), **4** (1.8 mg, t_R 43.9 min), **5** (1.5 mg, t_R 52.4 min), and **7** (2.8 mg, t_R 62.9 min) were obtained from fraction PLL3F (22.7 mg) by semipreparative RP-18 HPLC and eluted with ACN–H_2O (2 mL/min, 1:1, v/v). Fraction PLL3G (31.4 mg) was subjected to RP-18 HPLC eluted with ACN–H_2O (2 mL/min, 2:3, v/v) to give compounds **1** (1.4 mg, t_R 84.6 min) and **2** (0.9 mg, t_R 79.1 min).

4.3.1. Phaeanthuslucidine E (1)

Yellow amorphous powder: $[\alpha]_D^{25}$ −87 (*c* 0.01, MeOH); UV (MeOH) λ_{max} (log *ε*) 206 (4.2), 241 (3.9), 285 (3.9), and 324 (3.3); IR (neat) ν_{max} 3413, 2923, 1677, 1604, and 1457 cm^{-1}; ECD (MeOH) λ_{max} (Δε) 237 (−1.76), 273 (+0.49) nm; ^1H and ^{13}C NMR, see Table 1; HRESIMS *m/z* 446.1583 $[M + H]^+$ (calcd for $C_{26}H_{24}NO_6$, 446.1598).

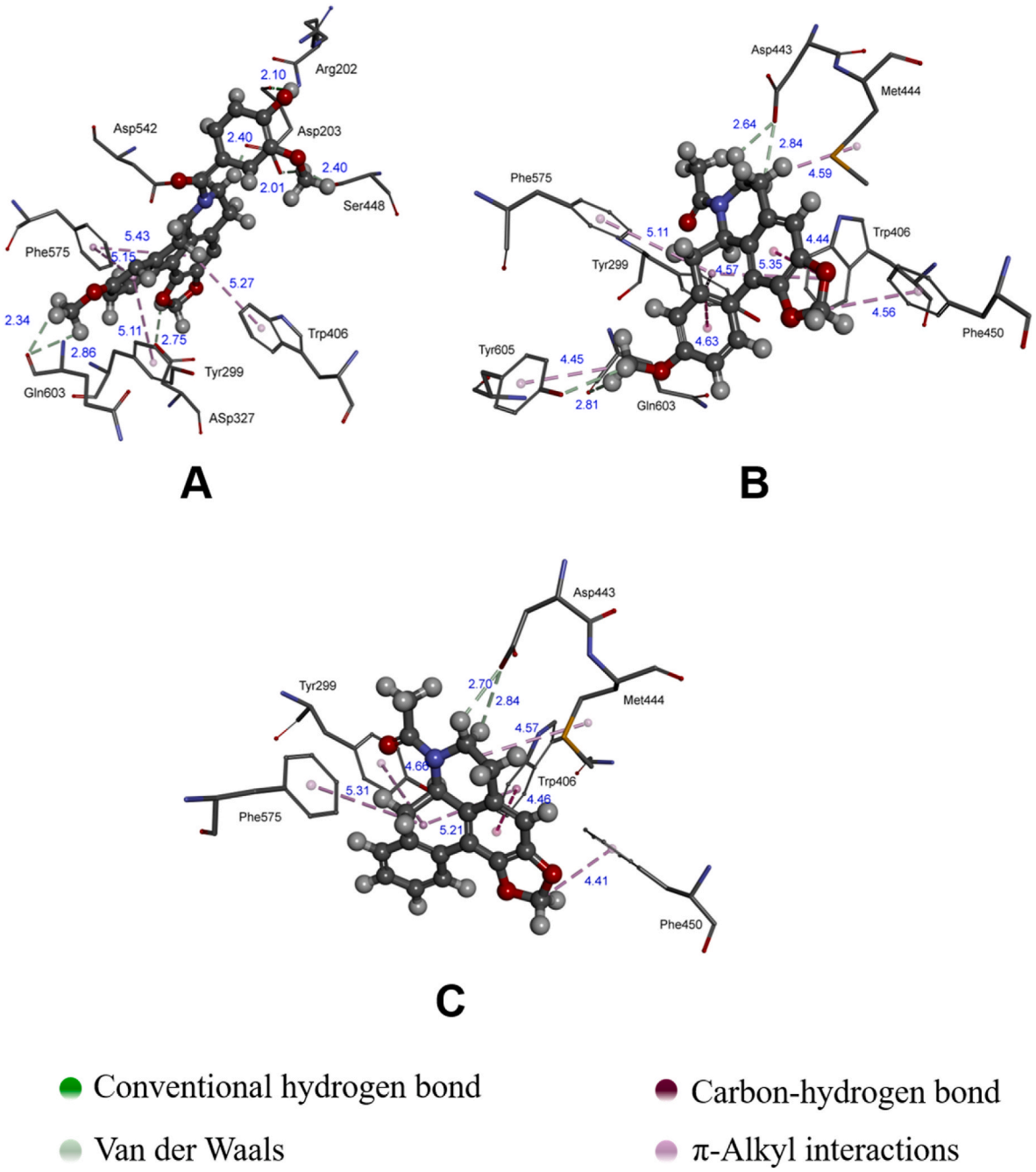

Fig. 5. 3D ligand interaction diagram of compounds **1** (A), **4** (B), and **5** (C) in the catalytic site of *α*-glucosidase.

4.3.2. *Phaeanthuslucidine F (2)*

Brown amorphous powder: $[\alpha]_D^{25}$ −43 (*c* 0.01, MeOH); UV (MeOH) λ_{max} (log *ε*) 213 (4.5), 267 (4.2), and 295 (3.9); IR (neat) ν_{max} 3393, 2924, 1648, 1603, and 1463 cm^{-1}; ECD (MeOH) λ_{max} (Δε) 210 (−1.57), 237 (−1.76), 278 (+0.38) nm; ^1H and ^{13}C NMR, see Table 1; HRESI-TOFMS *m/z* 476.1705 $[M + H]^+$ (Trg. for $C_{27}H_{25}NO_7$, 475.1631).

4.3.3. *Phaeanthuslucidine G (3)*

Yellow amorphous powder: $[\alpha]_D^{25}$ −56 (*c* 0.01, MeOH); UV (MeOH) λ_{max} (log *ε*) 222 (4.1), 256 (4.0), and 294 (3.7); IR (neat) ν_{max} 3380, 2921, 1665, 1595 and 1454 cm^{-1}; ECD (MeOH) λ_{max} (Δε) 231 (−1.61), 271 (+0.51) nm; ^1H and ^{13}C NMR, see Table 1; HRESITOFMS *m/z* 416.1494 $[M + H]^+$ (Trg. for $C_{25}H_{21}NO_5$, 415.1420).

4.3.4. *Phaeanthusnaphthoquinone (7)*

Yellow amorphous powder: UV (MeOH) λ_{max} (log *ε*) 234 (3.9), 276 (4.1), and 312 (3.7); IR (neat) ν_{max} 2927, 1724, 1647, 1519, 1454 and 1249 cm^{-1}; ^1H and ^{13}C NMR, see Table 2; HRESIMS *m/z* 295.0959 $[M + H]^+$ (calcd for $C_{18}H_{15}O_4$, 295.0965).

4.4. *α-Glucosidase inhibitory assay*

According to the previously published procedure with a slight modification (He et al., 2020; Hou et al., 2021), the *α*-glucosidase enzyme was prepared at 0.05 U/mL by dissolving with phosphate buffer (pH 6.8−7.0), then treated with the tested compounds at various concentrations (0.1−1000 μg/mL) at 37 °C for 10 min. The reaction was performed in 96-well plates using 1 mM of *p*-nitrophenyl *α*-D-glucopyranoside (*p*-NPG) as the substrate in phosphate buffer at 37 °C for 20

min. After 20 min, the reaction was terminated by adding 1 mL of 0.3 M Na_2CO_3. The hydrolyzation of *p*-NPG can be measured at 405 nm. Acarbose was used as a positive control.

4.5. Molecular docking study

The crystal structure of α-glucosidase [PDB entry code: 2QMJ] was obtained from the Protein Data Bank (http://www.rcsb.org/pdb). The structures of compounds were built with Gaussview and Gaussian 03 W was used for energy optimization. Auto Dock Tools 1.5.4 (ADT) and Auto Dock 4.2 programs were used for molecular docking with 50 runs. A grid box size of 60 × 60 × 60 points with a spacing of 0.375 Å between the grid points was implemented and covered almost the entire α-glucosidase protein surface (Kumboonma et al., 2021).

CRediT authorship contribution statement

Passakorn Teerapongpisan: Writing – review & editing, Writing – original draft, Investigation, Formal analysis, Data curation. **Virayu Suthiphasilp:** Writing – original draft, Formal analysis. **Pakit Kumboonma:** Writing – original draft, Resources, Investigation, Formal analysis. **Tharakorn Maneerat:** Writing – original draft, Resources, Data curation. **Thidarat Duangyod:** Writing – original draft, Resources, Data curation. **Rawiwan Charoensup:** Writing – original draft, Resources, Data curation. **Phunrawie Promnart:** Writing – review & editing, Writing – original draft, Data curation. **Surat Laphookhieo:** Writing – review & editing, Writing – original draft, Supervision, Project administration, Funding acquisition, Formal analysis, Data curation, Conceptualization.

Declaration of competing interest

The authors declare the following financial interests/personal relationships which may be considered as potential competing interests: Surat Laphookhieo reports financial support was provided by National Research Council of Thailand. Surat Laphookhieo reports a relationship with National Research Council of Thailand that includes: funding grants and travel reimbursement. If there are other authors, they declare that they have no known competing financial interests or personal relationships that could have appeared to influence the work reported in this paper.

Data availability

Data will be made available on request.

Acknowledgments

This work was supported by the National Research Council of Thailand (NRCT) and Mae Fah Luang University (N42A650373). We also thank Mr. Abdulromea Baka for plant identification.

Appendix A. Supplementary data

Supplementary data to this article can be found online at https://doi.org/10.1016/j.phytochem.2024.114020.

References

Atan, M.S., Dzulkefly, K.A., Aspollah, S.M., Anuar, K., Vijay, S., 2011. Isolation and antibacterial activity of alkaloids from Phaeanthus opthalmicus. Asian J. Chem. 23, 3824–3826.

Auranwiwat, C., Wongsomboon, P., Thaima, T., Rattanajak, R., Kamchonwongpaisan, S., Willis, A.C., Lie, W., Pyne, S.G., Limtharakul, T., 2017. 2-Phenylnaphthalenes and a polyoxygenated cyclohexene from the stem and root extracts of Uvaria cherrevensis (Annonaceae). Fitoterapia 120, 103–107. https://doi.org/10.1016/j.fitote.2017.06.002.

Chaichompoo, W., Rojsitthisak, P., Pabuprapap, W., Siriwattanasathien, Y., Yotmanee, P., Haritakun, W., Suksamrarn, A., 2021. Stephapierrines A–H, new tetrahydroprotoberberine and aporphine alkaloids from the tubers of Stephania pierrei Diels and their anti-cholinesterase activities. RSC Adv. 11, 21153–21169. https://doi.org/10.1039/D1RA03276C.

Chang, F.R., Chen, C.Y., Wu, P.H., Kuo, R.Y., Chang, Y.C., Wu, Y.C., 2000. New alkaloids from Annona purpurea. J. Nat. Prod. 63, 746–748. https://doi.org/10.1021/np990548n.

Chen, J.J., Hung, H.C., Sung, P.J., Chen, I.S., Kuo, W.L., 2011. Aporphine alkaloids and cytotoxic lignans from the roots of Illigera luzonensis. Phytochemistry 72, 523–532. https://doi.org/10.1016/j.phytochem.2010.12.015.

Guo, Z.F., Wang, X.B., Luo, J.G., Luo, J., Wang, J.S., Kong, L.Y., 2011. A novel aporphine alkaloid from Magnolia officinalis. Fitoterapia 82, 637–641. https://doi.org/10.1016/j.fitote.2011.01.021.

He, X.F., Chen, J.J., Li, T.Z., Zhang, X.K., Guo, Y.Q., Zhang, X.M., Hu, J., Geng, C.A., 2020. Nineteen new flavanol–fatty alcohol hybrids with α-glucosidase and PTP1B dual inhibition: one unusual type of antidiabetic constituent from Amomum tsao-ko. J. Agric. Food Chem. 68, 11434–11448. https://doi.org/10.1021/acs.jafc.0c04615.

Hou, Z.W., Chen, C.H., Ke, J.P., Zhang, Y.Y., Qi, Y., Liu, S.Y., Yang, Z., Ning, J.M., Bao, G.H., 2021. α-Glucosidase inhibitory activities and the interaction mechanism of novel spiro-flavoalkaloids from YingDe Green Tea. J. Agric. Food Chem. 70, 136–148. https://doi.org/10.1021/acs.jafc.1c06106.

Johns, S.R., Lamberton, K.A., Sioumis, A.A., 1968. Alkaloids of a Phaeanthus species from New Guinea. Isolation of phaeanthine and limacine. Aust. J. Chem. 21, 1387–1388. https://doi.org/10.1071/CH9681387.

Kumboonma, P., Senawong, T., Saenglee, S., Phaosiri, C., 2021. Discovery of new capsaicin and dihydrocapsaicin derivatives as histone deacetylase inhibitors and molecular docking studies. Org. Commun. 14, 133–143. https://doi.org/10.25135/acg.oc.102.21.03.1998.

Liu, Y., Li, Y., Muema, F.W., Zhang, H., Seukep, A.J., Guo, M., 2023. Aporphine alkaloids identified from Xylopia aethiopica and their potential hypoglycemic and hypolipidemic activities. J. Funct.Foods 106, 105601. https://doi.org/10.1016/j.jff.2023.105601.

Lo, W.L., Chang, F.R., Wu, Y.C., 2000. Alkaloids from the leaves of Fissistigma glaucescens. J. Chin. Chem. Soc. 47, 1251–1256. https://doi.org/10.1002/jccs.200000172.

Magpantay, H.D., Malaluan, I.N., Manzano, J.A.H., Quimque, M.T., Pueblos, K.R., Moor, N., Budde, S., Bangcaya, P.S., Valle, D.L., Dahse, H.M., Khan, A., Wei, D.Q., Alejandro, G.J.D., Macabeo, A.P.G., 2021. Antibacterial and COX-2 inhibitory tetrahydrobisbenzylisoquinoline alkaloids from the Philippine medicinal plant Phaeanthus ophthalmicus. Plants 10, 462. https://doi.org/10.3390/plants10030462.

Malaluan, I.N., Manzano, J.A.H., Muñoz, J.E.R., Bautista, T.J.L., Dahse, H.M., Quimque, M.T.J., 2022. Antituberculosis and antiproliferative activities of the extracts and tetrahydrobisbenzylisoquinoline alkaloids from Phaeanthus ophthalmicus: in vitro and in silico investigations. Philippine J. Sci. 151, 371–381.

Matsushige, A., Kotake, Y., Matsunami, K., Otsuka, H., Ohta, S., Takeda, Y., 2012. Annonamine, a new aporphine alkaloid from the leaves of Annona muricata. Chem. Pharm. Bull. 60, 257–259. https://doi.org/10.1248/cpb.60.257.

Nguyen, N.T., Pham, V.C., Litaudon, M., Gueritte, F., Grellier, P., Nguyen, V.T., Nguyen, V.H., 2008. Antiplasmodial alkaloids from Desmos rostrata. J. Nat. Prod. 71, 2057–2059. https://doi.org/10.1021/np8004437.

Nhiem, N.X., Tuong, N.T., Ky, P.T., Subedi, L., Park, S.J., Ngoc, T.M., Yen, P.H., Tai, B.T., Quang, T.H., Kim, S.H., 2017. Chemical components from Phaeanthus vietnamensis and their inhibitory NO production in BV2 cells. Chem. Biodivers. 14, e1700013 https://doi.org/10.1002/cbdv.201700013.

Nonato, M.G., Garson, M.J., Truscott, R.J., Carver, J.A., 1990. ^{1}H-NMR assignments of anonaine and xylopine derivatives from Talauma gitingensis. J. Nat. Prod. 53, 1623–1627. https://doi.org/10.1021/np50072a043.

Pabon, L.C., Cuca, L.E., 2010. Aporphine alkaloids from Ocotea macrophylla (Lauraceae). Quim. Nova 33, 875–879. https://doi.org/10.1590/S0100-40422010000400021.

Ringdahl, B., Chan, R.P., Craig, J.C., Cava, M.P., Shamma, M., 1981. Circular dichroism of aporphines. J. Nat. Prod. 44, 80–85. https://doi.org/10.1021/np50013a014.

Salae, A.W., Chairerk, O., Sukkoet, P., Chairat, T., Prawat, U., Tuntiwachwuttikul, P., Chalermglin, P., Ruchirawat, S., 2017. Antiplasmodial dimeric chalcone derivatives from the roots of Uvaria siamensis. Phytochemistry 135, 135–143. https://doi.org/10.1016/j.phytochem.2016.12.009.

Sedmera, P., Nghia, N.T., Valka, I., Cave, A., Cortes, D., Simanek, V., 1990. A new bisbenzylisoquinoline alkaloid from Phaeanthus vietnamensis and its antibacterial activity. Heterocycles 30, 205–209. https://doi.org/10.3987/COM-89-S2.

Teerapongpisan, P., Suthiphasilp, V., Kumboonma, P., Maneerat, T., Duangyod, T., Charoensup, R., Andersen, R.J., Laphookhieo, S., 2023. Phaeanthuslucidines A–D, dimeric aporphine alkaloid derivatives from Phaeanthus lucidus Oliv. Phytochemistry 212, 113717. https://doi.org/10.1016/j.phytochem.2023.113717.

Tsai, T.H., Wang, G.J., Lin, L.C., 2008. Vasorelaxing alkaloids and flavonoids from Cassytha filiformis. J. Nat. Prod. 71, 289–291. https://doi.org/10.1021/np070564h.

Tu, D.N., Hau, V.T.B., Diep, N.T., Khanh, H.V., Long, N.T., Trang, H.T.H., Hoang, N.H., Kiem, P.V., Nhiem, N.X., 2022. Alkaloids from Phaeanthus vietnamensis with inhibitory effect on nitric oxide production lipopolysaccharide-stimulated in RAW264.7 macrophages. J. Asian Nat. Prod. Res. 24, 898–903. https://doi.org/10.1080/10286020.2021.1993833.

Wiya, C., Aongyong, K., Damthongdee, A., Baka, A., Chaowasku, T., 2021. The genus Phaeanthus (Annonaceae, Miliuseae) in Thailand: P. piyae sp. nov. and resurrection of P. lucidus, with molecular phylogenetic analyses. Taiwania 66, 371–381. https://doi.org/10.6165/tai.2021.66.509.

Wu, S.F., Hwang, T.L., Chen, S.L., Wu, C.C., Ohkoshi, E., Lee, K.H., Chang, F.R., Wu, Y.C., 2011. Bioactive components from the heartwood of Pterocarpus santalinus. Bioorg. Med. Chem. Lett. 21, 5630–5632. https://doi.org/10.1016/j.bmcl.2011.06.036.

Yu, H.J., Chen, C.C., Shieh, B.J., 1998. The constituents from the leaves of Magnolia coco. J. Chin. Chem. Soc. 45, 773–778. https://doi.org/10.1002/jccs.199800116.

Yu, Z., Han, C., Song, X., Chen, G., Chen, J., 2019. Bioactive aporphine alkaloids from the stems of Dasymaschalon rostratum. Bioorg. Chem. 90, 103069 https://doi.org/10.1016/j.bioorg.2019.103069.

Zaima, K., Takeyama, Y., Koga, I., Saito, A., Tamamoto, H., Azziz, S.S.S.A., Mukhtar, M. R., Awang, K., Hadi, A.H.A., Morita, H., 2012. Vasorelaxant effect of isoquinoline derivatives from two species of Popowia perakensis and Phaeanthus crassipetalus on rat aortic artery. J. Nat. Med. 66, 421–427. https://doi.org/10.1007/s11418-011-0600-4.

Zheng, Y.K., Su, B.J., Wang, Y.Q., Wang, H.S., Liao, H.B., Liang, D., 2021. New tyramine- and aporphine-type alkamides with NO release inhibitory activities from Piper puberulum. J. Nat. Prod. 84, 1316–1325. https://doi.org/10.1021/acs.jnatprod.1c00055.